

Article

Evaluating the Rheological, Chemical and Morphological Properties of SBS Modified Asphalt-Binder under Multiple Aging and Rejuvenation Cycles

Xiaobing Chen ^{1,*}, Yunfeng Ning ^{1,*} , Yongming Gu ², Ronglong Zhao ¹, Jinhu Tong ¹, Juntian Wang ³, Xiaorui Zhang ¹  and Wei Wen ¹

¹ School of Transportation, Southeast University, Nanjing 211189, China; along@seu.edu.cn (R.Z.); 101010035@seu.edu.cn (J.T.); zxr@seu.edu.cn (X.Z.); 220203258@seu.edu.cn (W.W.)

² Suzhou Communications Investment Group Co., Ltd., Suzhou 215004, China; szgtsn@sina.com

³ Hangzhou Transportation Development Support Center, Hangzhou 310030, China; 220183082@seu.edu.cn

* Correspondence: xbchen@seu.edu.cn (X.C.); 220193090@seu.edu.cn (Y.N.)

Featured Application: This paper presents the trends in the rheological, chemical, and morphological properties of SBS-modified asphalt-binders under multiple cycles of aging and rejuvenation. The results from this study may provide guidance for the future development of rejuvenators and application of repeated penetrating rejuvenation.



Citation: Chen, X.; Ning, Y.; Gu, Y.; Zhao, R.; Tong, J.; Wang, J.; Zhang, X.; Wen, W. Evaluating the Rheological, Chemical and Morphological Properties of SBS Modified Asphalt-Binder under Multiple Aging and Rejuvenation Cycles. *Appl. Sci.* **2021**, *11*, 9242. <https://doi.org/10.3390/app11199242>

Academic Editors: Amir Tabakovic, Jan Valentin and Liang He

Received: 31 August 2021

Accepted: 1 October 2021

Published: 4 October 2021

Publisher's Note: MDPI stays neutral with regard to jurisdictional claims in published maps and institutional affiliations.

Abstract: To investigate the influence of multiple cycles of aging and rejuvenation on the rheological, chemical, and morphological properties of styrene–butadiene–styrene (SBS)-modified asphalt-binders, the asphalt-binders were aged using two laboratory simulation methods, namely a rolling thin film oven (RTFO) test for short-term aging and pressure aging vessel (PAV) for long-term aging. The asphalt-binders were then rejuvenated with three types of rejuvenators (Type I, II, and III) with different dosages (i.e., 6%, 10%, and 14% for the first, second, and third rejuvenation, respectively). A dynamic shear rheometer (DSR) was then used to analyze the effect of rejuvenators on the rheological properties of all the asphalt-binders. The changes in the functional groups and microscopic morphology in the process of multiple aging and rejuvenation cycles were studied using Fourier transform infrared (FTIR) and atomic force microscopy (AFM). The results indicated that the three rejuvenators could soften the stiffness and restore the microstructures of the aged asphalt-binders in the process of repeated aging and rejuvenation from DSR and AFM testing. Considering the rutting and fatigue properties, the Type I rejuvenator exhibited the potential to achieve the desired rejuvenation effects under multiple rejuvenation cycles. During the multiple aging and rejuvenation cycles, the aging resistance of SBSMA decreased gradually from the FTIR results. This inherently limited the number of repeated rejuvenation cycles. This research is conducive to promoting the application of repeated penetrating rejuvenation.

Keywords: multiple aging and rejuvenation cycles; SBS modified asphalt; morphological properties; DSR; FTIR; AFM



Copyright: © 2021 by the authors. Licensee MDPI, Basel, Switzerland. This article is an open access article distributed under the terms and conditions of the Creative Commons Attribution (CC BY) license (<https://creativecommons.org/licenses/by/4.0/>).

1. Introduction

Due to the mature production process, cost-effectiveness, and the outstanding performance in terms of rutting, cracking, and moisture resistance, styrene–butadiene–styrene-modified asphalt-binder (SBSMA) is one of the most commonly used asphalt-binders for pavement construction, particularly as a surfacing layer [1]. The principle idea is to take advantage of the good binding and hardening properties of the SBS polymer to achieve effective modification of the bituminous material [2]. Thus, SBSMA has broad market prospects and accounts for more than 50% of the modified asphalt-binder around the world [3].

Nevertheless, SBSMA is inevitably prone to aging during the service life of the pavement as a result of the negative effects of oxygen, heat, and ultraviolet (UV) light, which ultimately lead to the hardening and embrittlement of the asphalt-binder [4,5]. These effects usually result in the degradation of the SBS polymer and oxidation along with the volatilization of light components and the polycondensation of the asphalt-binder, consequently causing a decay in the physico-rheological properties [6–8]. Many researchers have observed an increase in the complex modulus (G^*), elastic modulus (G'') and creep recovery (R), but a reduction in phase angle (δ) and non-recoverable creep compliance (J_{nr}) with the deepening of the aging by DSR, which means that the viscous behavior of the asphalt-binder has partly moved to elastic behavior [9–11].

SBSMA's performance decay accelerates pavement distresses and shortens its service life under traffic loading and fluctuating environmental conditions. It is essential to make a proper decision to restore the physico-rheological properties of the asphalt-binder at an appropriate time during the life cycle of the pavement [12]. Therefore, rejuvenators are often added to aged asphalt-binders to soften them and make the rejuvenated asphalt-binders more fluid. Specifically, the effects of the rejuvenators on the asphalt-binders include an increase in the penetration grade, ductility, phase angle, m -value, and a corresponding decrease in the softening point, viscosity, shear complex modulus, rutting factor, and stiffness, respectively [13,14].

During the aging and rejuvenation processes, the change in the physico-rheological properties of the SBSMA can be attributed to the chemical composition and microstructures. Fourier transform infrared (FTIR), atomic force microscopy (AFM), environmental scanning electron microscope (ESEM), and other new technologies have been successfully applied to analyze the aging mechanism and rejuvenating process of SBSMA at a micro scale [11,15–25]. FTIR was used to investigate the aging and rejuvenation mechanism of SBSMA as well as the relationship between the chemical and rheological characteristics by identifying the differences between the absorption peaks which represent the functional groups and contents in the asphalt-binder based on Lambert–Beer's Law [15–18]. Yang et al. [20] found that the oxygen content of the asphalt-binder increased greatly after thermal aging, leading to an increase in the polar functional groups such as carbonyl and sulfoxide groups in the asphalt-binder. In terms of rejuvenation, rejuvenators regularly decreased the carbonyl and sulfoxide indices [21]. The AFM can obtain the microscopic morphology of the asphalt-binder surface [10]. Guo et al. [22] observed that the bee structures slightly increased after PAV aging, and rejuvenator made the microstructures larger. Ozdemir et al. [23] studied aging effects of varying processing parameters on the phase structure of SBSMA. Cong et al. [24] observed a decrease in the surface roughness with aging. Aghazadeh Dokandari et al. [25] observed that tiny bee structures appeared with the addition of the rejuvenator.

The rejuvenation of aged SBSMA and reuse of asphalt mixtures reduces the environmental impacts, such as land occupation and consumption of nonrenewable resources [4]. Rapid in-place pavement recycling at an appropriate time is a very promising technology for preventive maintenance, and has an advantage of time- and cost-efficiency [26]. However, one cycle of rejuvenation has become inadequate to meet the current environmental and traffic demands. Considering the availability of bitumen and its price uncertainty, the need for multiple instances of maintenance in road construction has become essential. Three or four instances of maintenance has been proposed to extend the service life by 10–15 years with over 50% cost savings [12].

With the above background, it is therefore imperative to conduct a laboratory study on the multiple aging and rejuvenation cycles of asphalt-binder where rejuvenated asphalt-binder is widely used. Furthermore, multiple-cycle rejuvenation is expected to be a common practice in the future. To explore the mechanisms of multiple cycle aging and rejuvenation, various technological methods including FTIR and AFM were applied in this study for quantitatively evaluating the chemical and morphological properties of SBSMA through repeated aging and rejuvenation laboratory testing. Another aim of this study

was to investigate the effects of multiple aging and rejuvenation cycles on the rheological parameters of SMSMA and the potential for repeated rejuvenation of flexible pavements, so laboratory experimentations were accomplished by using DSR for investigating.

2. Materials and Test Methods

SBSMAs were separately blended with three types of rejuvenators at different dosages in multiple aging and rejuvenation cycles. Basic performance tests, namely DSR, FTIR, and AFM, were used to test the original, aged, and rejuvenated asphalt-binder samples. The high-temperature rutting parameters and intermediate-temperature fatigue parameters were obtained using the DSR test device [27]. The functional group changes of the asphalt-binder samples were obtained by analyzing the results from FTIR [20]. The microstructures of asphalt-binder samples were observed and characterized with AFM [10].

2.1. Materials

The main materials used in this study were asphalt-binder and three types of rejuvenators, namely Type I, Type II, and Type III, respectively.

2.1.1. Asphalt-Binder

The physical properties of the SBS-modified asphalt-binder (SBSMA) used in this study were acquired from SHELL Co., Ltd. The physical properties of SBSMA are listed in Table 1.

Table 1. Technical indices of SBS modified asphalt-binder (SBSMA).

Technical Index	Unit	Virgin	RTFO Residue	PAV Residue	Test Method
Penetration (25 °C, 100 g, 5 s)	0.1 mm	50.6	35.0	22.4	ASTM D5
Softening point, $T_{R\&B}$	°C	78.9	81.0	83.2	ASTM D36
Ductility (5 °C, 5 cm/min)	cm	25.2	14.7	2.0	ASTM D113

2.1.2. Rejuvenators

The three different types of rejuvenators were asphaltene-free cationic rejuvenating emulsions fabricated from petroleum-based oil. The principal properties and infrared spectra of the three rejuvenators used are listed in Table 2 and shown in Figure 1, respectively, all indicating nearly similar components and chemical structures.

2.2. Experimental Design Plan

Laboratory short-term aging was carried out using the rolling thin-film oven test (RTFO, 163 °C, 1.0 MPa, 85 min) to simulate aging during storage, mixing, transport, and placing. Thereafter, the pressurized aging vessel test (PAV, 100 °C, 2.1 MPa, 20 h) was performed to roughly simulate 5 years of field aging [28] in accordance with ASTM D2872 [29] and ASTM D6521 [30]. The virgin SBSMA was subjected to RTFO and PAV aging to obtain the first aged SBSMA.

Table 2. Technical indices of the rejuvenators.

Technical Index	Unit	Type I	Type II	Type III	Test Method
Viscosity @25 °C	SFS	25~150	20~60	25~150	ASTM D7496
Residue	%	>64	60~65	>65	ASTM D6934
Particle charge	—	Positive	Positive	Positive	ASTM D7402
Asphaltenes	%	<11.5	2~4	<11	ASTM D2006
Maltene distribution ratio (PC+A ₁)/(S+A ₂) ¹	—	0.8~1.4	0.5~0.9	0.7~1.1	ASTM D2006
PC/S ratio	—	>1.2	>1.2	>0.5	ASTM D2006

¹ PC = Polar Compound; A₁ = First Acidaffins; A₂ = the Second Acidaffins; S = Saturated Hydrocarbons.

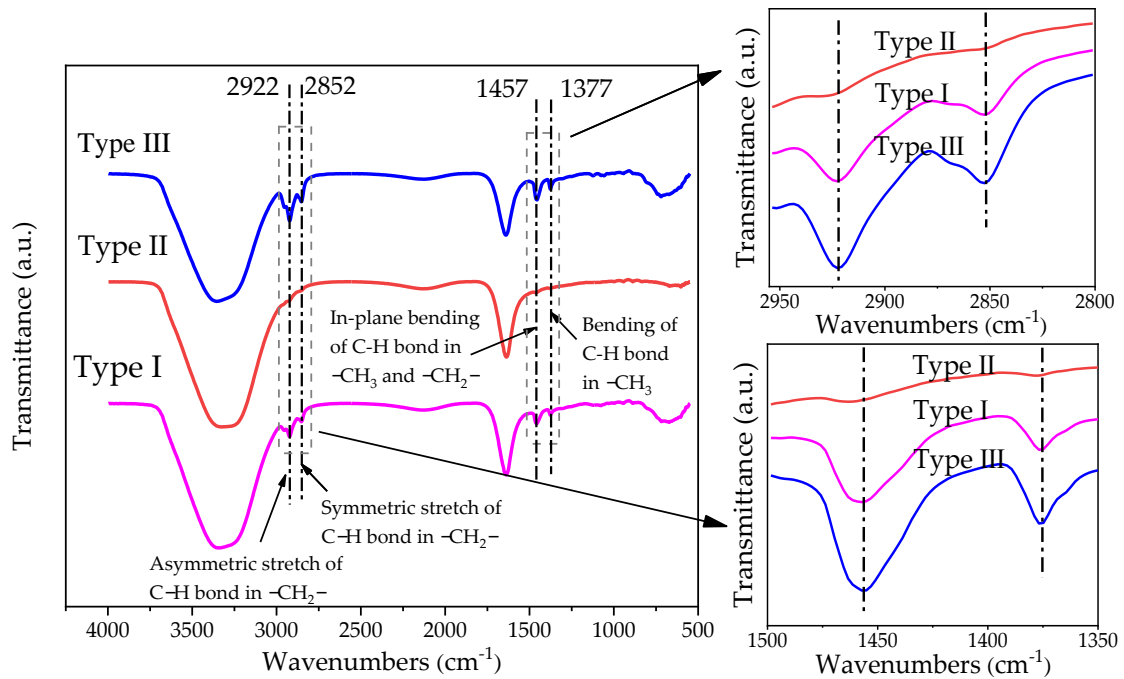


Figure 1. FTIR spectra of the three rejuvenators.

For the purpose of investigating the influence of multiple aging and rejuvenation cycles on the SBSMA in the field, 6%, 10%, and 14% by weight (wt%) of the asphalt-binder were selected as the rationale dosage of the rejuvenator for the first, second, and third rejuvenation, respectively, in accordance with previous research studies [26]. The first aged SBSMA was heated to 140~160 °C for melting and blended with three rejuvenators for 30 min to prepare the first rejuvenated SBSMA. Thereafter, the first rejuvenated SBSMA was directly placed in the PAV (100 °C, 2.1 MPa, 20 h) for long-term aging (rather than RTFO first) to obtain the second aged asphalt-binder on account of the in-place penetrating rejuvenation without the need for heated construction. The second rejuvenated asphalt-binder was prepared by adding 10 wt% of the rejuvenator to the second aged SBSMA. The third aged asphalt-binder and the third rejuvenated asphalt-binder were obtained by the same method. Figure 2 illustrates the experimental design plan for this research study.

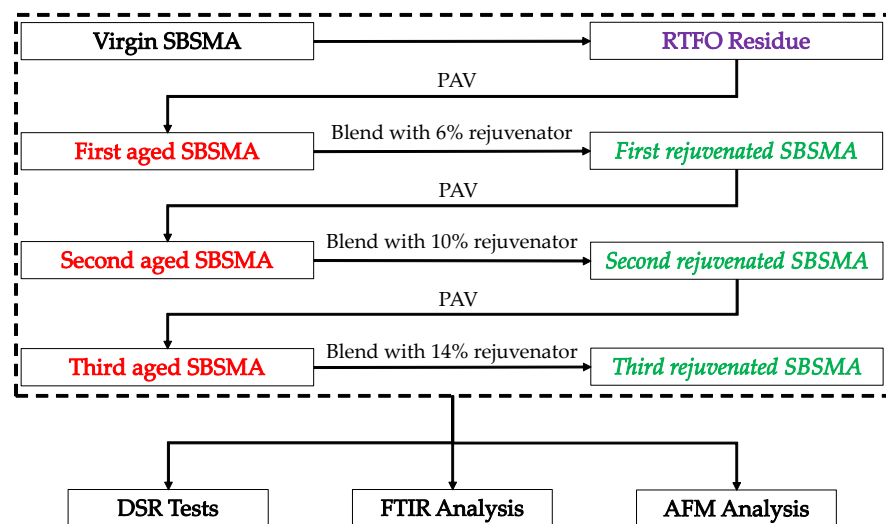


Figure 2. Experimental flow chart.

2.3. Laboratory Testing

2.3.1. Rheological Property Tests

The dynamic rheological properties of the SBSMA at different cycles of aging and rejuvenation were measured using the DSR test device (Kinexus Pro+, Malvern, Wolverhampton, UK).

Temperature sweep tests were carried out under the strain-controlled loading mode at a constant frequency of $10 \text{ rad}\cdot\text{s}^{-1}$ in accordance with the ASTM D7405 [31]. The temperature range was $58\text{--}82 \text{ }^\circ\text{C}$ for the rejuvenated asphalt-binders, and $22\text{--}34 \text{ }^\circ\text{C}$ for the aged asphalt-binders. The applied strain levels for the temperature sweep tests were controlled in the linear viscoelastic range. The rejuvenated asphalt-binder samples were molded to a diameter of 25 mm by 1 mm thick whilst the aged asphalt-binder samples to a diameter of 8 mm by 2 mm thick.

Multiple Stress Creep Recover (MSCR) tests were conducted at $76 \text{ }^\circ\text{C}$ in line with the ASTM D7405 [31] test specification at standard stress levels of 0.1 kPa and 3.2 kPa, respectively. After subjecting the asphalt-binder samples to 10 loading cycles, each level with a 1 s loading period followed by a 9 s recovery period, two major rheological parameters, namely the percentage recovery (R) and non-recoverable creep compliance (J_{nr}), were calculated automatically at both stress levels of the DSR test.

Linear Amplitude Sweep (LAS) tests were performed using the DSR test device with 8 mm parallel plates and 2 mm gap to determine the asphalt-binders' resistance to fatigue damage in accordance with the AASHTO T391-20 [32] test specification. The LAS test procedure consisted of two phases. Firstly, the frequency sweep test was performed at 0.1% strain level with a frequency range of 0.1~30 Hz to obtain the undamaged property of the samples (α). Then, in the amplitude sweep, the load was applied from 0 to 30% strain at 10 Hz for 300 s under strain-controlled loading mode. The LAS test data were processed using a Visco-Elastic Continuum Damage (VECD) model approach to determine the fatigue parameters A and B. In this study, all the LAS tests were performed at a room temperature of $25 \text{ }^\circ\text{C}$.

2.3.2. FTIR Tests

FTIR tests were performed using a Bruker Alpha FTIR spectrometer (Germany) equipped with a reflection diamond ATR accessory to analyze the functional groups of samples qualitatively or quantitatively with an accumulation of 32 scans in a $400\text{--}4000 \text{ cm}^{-1}$ range and a resolution of 4 cm^{-1} (Figure 3a). The samples were directly placed on a zinc selenide horizontal ATR crystal, which should be totally cleaned using kerosene and alcohol after each test operation [33]. The raw FTIR data were processed and analyzed using a software program called OPUS.



(a)



(b)

Figure 3. Microscopic analysis equipment: (a) FTIR-ATR; (b) AFM.

2.3.3. AFM Tests

Atomic force microscopy (AFM, Bruker Dimension ICON, USA) was used to investigate the micro-morphology of the asphalt-binder at different cycles of aging and rejuvenation using the tapping mode (see Figure 3b). Because of the AFM requirement for a smooth surface of the sample molded, all the asphalt-binder samples for the AFM tests were prepared using the thermal method. This was necessary to avoid toxic solvents from dissolving and damaging the microstructures of the asphalt-binder [10].

A hot liquid drop of asphalt-binder (160 °C) was placed on a 10 × 10 × 2 mm glass substrate and put into the oven at a constant temperature of 145 °C for about 5 min and thereafter, cooled to the ambient temperature. The AFM samples with a flat and smooth surface were obtained and then moved to a closed dust-free container for storage before AFM observations.

Height and Z-images were scanned using an etched silicon probe. The probe (NANOSEN-SORTM, PPP-NCL-20) was used under the tapping mode. All the experiments were conducted at a temperature of 25 °C. The scanning range of 10 × 10 μm was used for the microstructure of the sample surfaces, and the range of 30 × 30 μm for analysis of the morphology was deemed a good statistical representation of the overall asphalt-binder samples.

2.3.4. Sample Replicates

For each rejuvenator type, content, aging condition, and test type, three sample replicates were tested. Overall, a total of 261 asphalt-binder samples (153 samples for the DSR tests, 54 samples for the FTIR tests, and 54 samples for the AFM tests) were prepared and tested.

3. Test Results, Analyses, and Discussion

3.1. Rheological Properties

The rheological properties of the asphalt-binders from the DSR test were used to evaluate the high-temperature rutting resistance and intermediate-temperature fatigue resistance of the modified asphalt-binder in the process of multiple aging and rejuvenation cycles. The specific DSR test results are presented and discussed below.

3.1.1. Temperature Sweep Analysis

The DSR temperature sweep tests were conducted with an isochronal plot to evaluate the temperature sensitivity of the asphalt-binder. The complex shear modulus (G^*) and phase angle (δ) were measured for subsequent computation of the analyzed rutting factor ($G^*/\sin\delta$) and fatigue factor ($G^*\cdot\sin\delta$).

The rutting factor ($G^*/\sin\delta$) reflects the deformation resistance of asphalt-binders at high temperatures [21]. Asphalt-binders with larger rutting factors have better rutting resistance at high temperatures. Figure 4 shows that the $G^*/\sin\delta$ values of the rejuvenated asphalt-binders decreased with an increase in temperature, and that the logarithm of $G^*/\sin\delta$ had a linear correlation with temperature.

After the second rejuvenation cycle, the $G^*/\sin\delta$ values of the asphalt-binders with Type I and Type III rejuvenators were comparatively close to those of the RTFO residue. However, only the third rejuvenated SBSMA with Type I rejuvenator had a $G^*/\sin\delta$ that was approximately equivalent to that of the RTFO residue. The superiority rank order of the rutting factors of the first, second, and third rejuvenated asphalt-binders was Type II > Type I > Type III, respectively. With an increase in the rejuvenation cycles, the rutting factor of the rejuvenated asphalt-binder with the Type II rejuvenator increased steadily, while that with the Type III rejuvenator decreased. Notably, the rutting factor of the aged SBSMA could be rejuvenated close to that of the RTFO residue by adding the Type I rejuvenator.

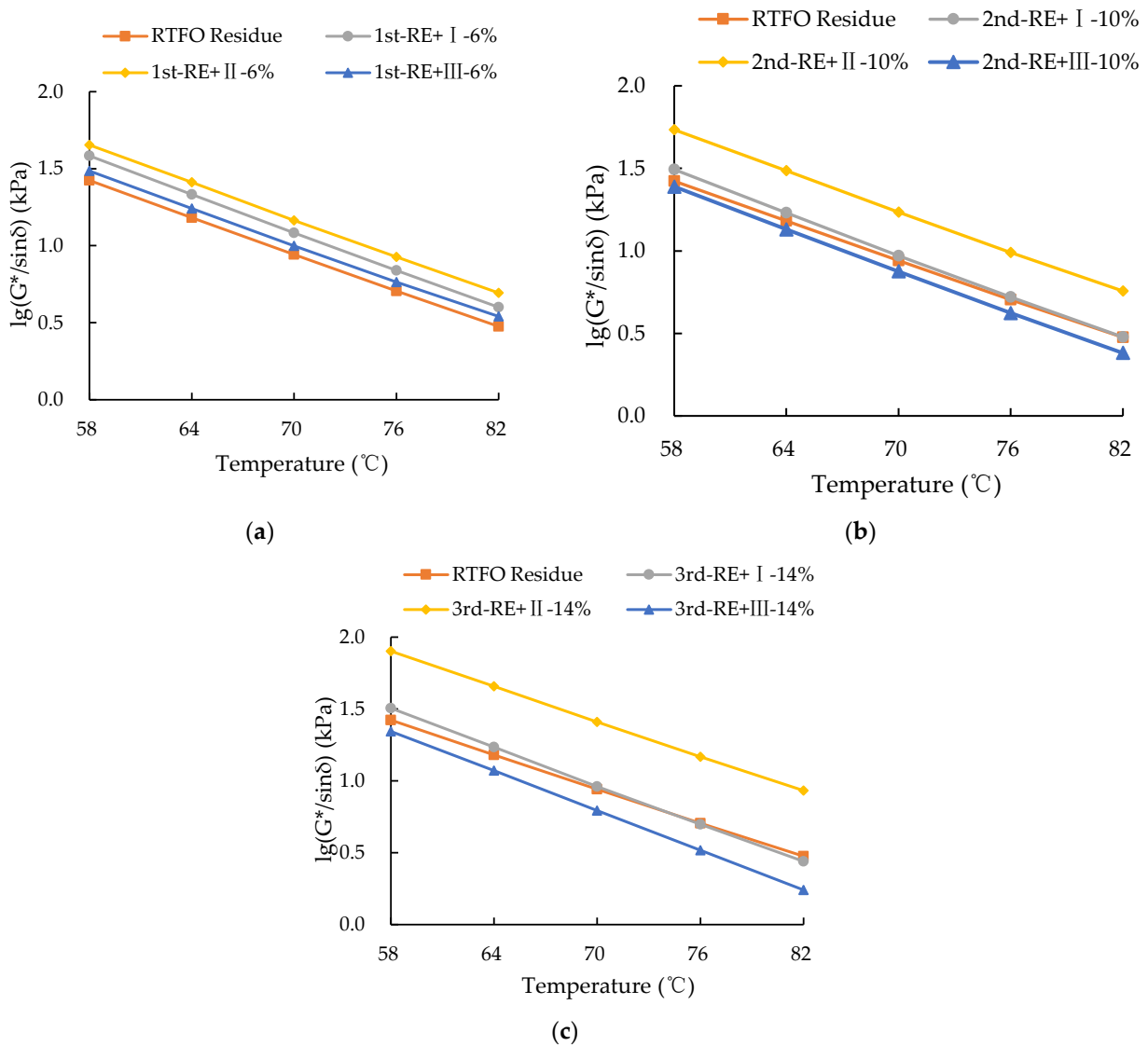


Figure 4. Rutting factor of SBS asphalt-binders at different rejuvenation cycles: (a) First cycle; (b) Second cycle; (c) Third cycle.

As the rejuvenation cycles increased, the dispersion of the rutting factor increased, indicating that repeated rejuvenation had a great influence on asphalt-binder’s rutting resistance. In general, the following was observed: (a) Type II rejuvenator enhanced the rutting resistance of the asphalt-binder, (b) Type III rejuvenator exhibited the potential to reduce the rutting resistance, and (c) Type I rejuvenator indicated the potential to help maintain the rutting resistance of the rejuvenated asphalt-binder.

The fatigue factor ($G^* \cdot \sin \delta$) reflects the anti-fatigue property of the asphalt-binder at intermediate temperatures [21]. Figure 5a,b show that the fatigue factors of the aged asphalt-binders decreased with an increase in temperature, and that the logarithm of $G^* \cdot \sin \delta$ had a linear correlation with temperature. The $G^* \cdot \sin \delta$ values of the second aged asphalt-binders with the three rejuvenators were close to that of the first aged asphalt-binder, whereas only the third aged SBSMA with Type I rejuvenator had nearly the same values as that of the PAV residue.

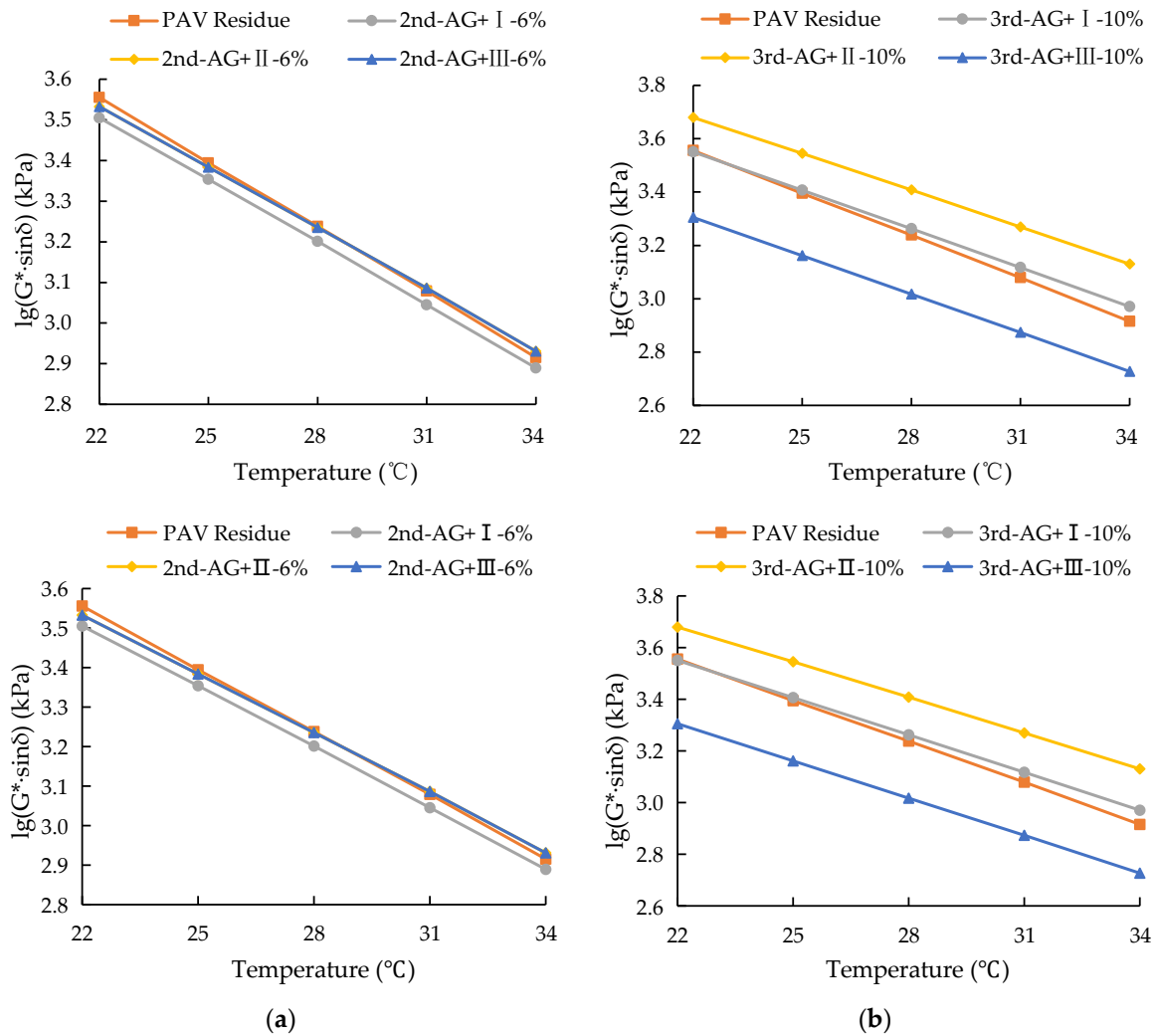


Figure 5. Fatigue factor of SBS asphalt-binders at different aging cycles: (a) Second cycle; (b) Third cycle.

From Figure 5, the fatigue factors of the third aged asphalt-binders ranked as follows: Type II > Type I > Type III. The fatigue property of the third aged asphalt-binders with the Type I rejuvenator was closest to that of the PAV residue, whilst that with the Type II rejuvenator was deemed as poor. The Type III rejuvenator, on the other hand, was found to be satisfactory and better than the other two types in terms of potential for fatigue resistance.

It was interesting to note that the widest dispersion of the fatigue factor was produced by the third aged asphalt-binders, followed by the second aged asphalt-binders as shown in Figure 5, indicating that the repeated aging process had a great influence on the rheological properties of the SBSMA. By comparison, the fatigue factor of the second and third aged asphalt-binders with the Type I rejuvenator were seen to be close to those of the PAV residue. This observation suggested that the expected rejuvenation performance can be achieved by blending with the Type I rejuvenator.

Theoretically, low continuous grade of the asphalt-binders at high temperature means poor high-temperature rutting resistance. As the number of rejuvenating cycles increased, the high-temperature continuous grade of SBSMA with Type I and III rejuvenators decreased continuously, while the grade of the asphalt-binder with Type II rejuvenator maintained an increasing trend. After the third cycle of rejuvenation, with an increase in high temperature, the grade of the asphalt-binder with Type II demonstrated an insufficient effectiveness of the repeated rejuvenation with Type II. By contrast, Type I and III rejuvenators could be applied to the repeated rejuvenation of SBSMA to reduce its high temperature grade. However, the grade reduction associated with the Type I rejuvenator

was relatively low. On the other hand, whilst the third rejuvenated asphalt-binder reached 84.1 °C, the third rejuvenated asphalt-binder with Type III was only 79.8 °C (see Figure 6a).

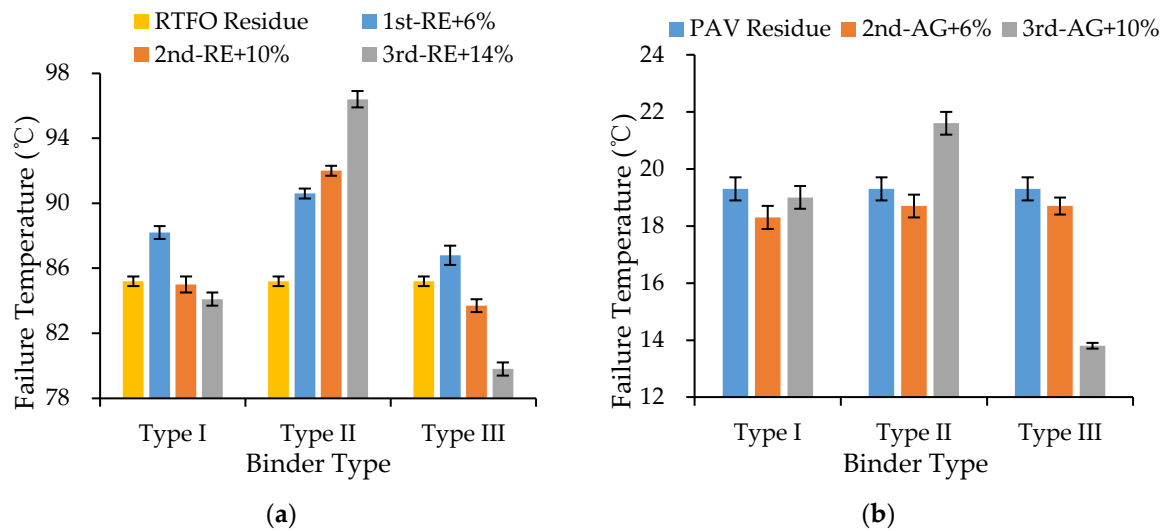


Figure 6. Failure temperature of SBS asphalt-binders at different aging and rejuvenation cycles: (a) High-temperature continuous grade; (b) intermediate-temperature continuous grade.

For asphalt-binders rejuvenated with Type I and II rejuvenators, the intermediate temperature continuous grade decreased to 18.3 °C and 18.7 °C (Type I and Type II, respectively), and then increased by 19.0 °C and 21.6 °C (Type I and Type II, respectively) with an increase in the number of aging cycles. For the asphalt-binders rejuvenated with Type III, the continuous grade at the intermediate temperature decreased with the aging cycles (see Figure 6b). The continuous grading temperature of the first, second, and third aged asphalt-binders rejuvenated with Type I were extremely close, showing that the fatigue properties of SBSMA rejuvenated with Type I could satisfactorily reach the virgin asphalt-binder level. Based on the results of the rutting and fatigue behavior of the asphalt-binders in different aging and rejuvenation cycles, Type I was considered to achieve the expected rejuvenation effects among the three types of rejuvenators evaluated.

3.1.2. MSCR Analysis

Percentage recovery (R), which reflects the recovery deformation for a period of ten creep and recovery cycles at each stress level, represents the elastic recovery performance of an asphalt-binder [34]. The larger percent recovery (R) indicates better rutting resistance of asphalt-binders [35]. Figure 7a shows the recovery response of the rejuvenated SBSMA with different rejuvenators at different rejuvenation cycles measured at 0.1 kPa and 3.2 kPa stress levels, respectively.

From Figure 7, it is evident that as the rejuvenation cycles increased, the percentage recovery of the asphalt-binder decreased under the same stress level. This meant a decline in the percentage recovery ability of the asphalt-binders after rejuvenation and the conversion promotion of the rejuvenators to the viscous component of the asphalt-binder. The percentage recovery of the third rejuvenated asphalt-binder with the Type III rejuvenator was 25.62% (3.2 kPa), which compared to the RTFO residue and the third rejuvenated asphalt-binder with Type II, represents a reduction factor of three. At the same stress level, the superiority ranking of the percentage recovery of SBSMA after similar rejuvenation cycles was Type II > Type I > Type III.

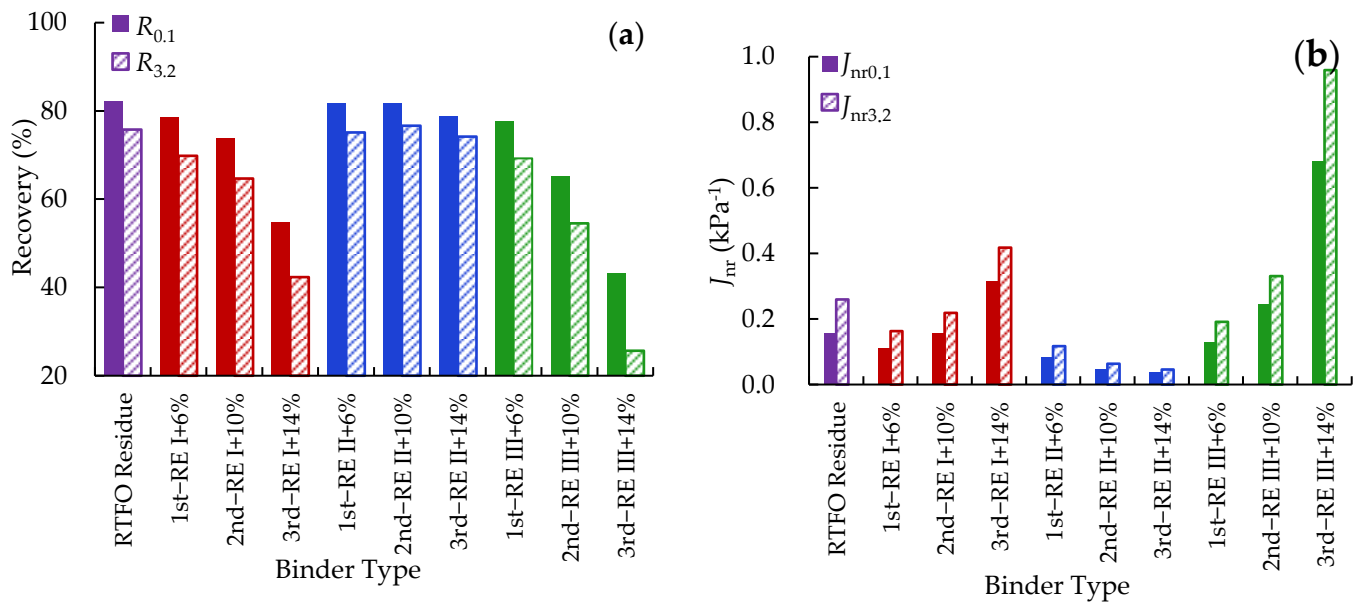


Figure 7. MSCR rutting evaluation of the repetitively rejuvenated asphalt-binders: (a) Recovery; (b) non-recoverable creep compliance (J_{nr}) (Red bars: the asphalt-binders rejuvenated with Type I; blue bars: the asphalt-binders rejuvenated with Type II; green bars: the asphalt-binders rejuvenated with Type III).

The non-recoverable creep compliance (J_{nr}) reflects the residual strain level of asphalt-binders after the loading-recovery cycle, which represents the rutting resistance of asphalt-binder. With an increased number of rejuvenation cycles, the rejuvenated asphalt-binders with Type I and Type III rejuvenators exhibited an increasing trend in the J_{nr} value and the non-recoverable strain at the same stress level (see Figure 7b). This implies a continuous drop in the rutting resistance. Particularly, the $J_{nr0.1}$ and $J_{nr3.2}$ values of the third rejuvenated asphalt-binder with Type III reached 0.684 kPa^{-1} and 0.959 kPa^{-1} , over 3 times the corresponding values of the RTFO residue. On the contrary, the rejuvenated asphalt-binder with Type II exhibited a continuously decreasing trend, indicating an improvement in the rutting resistance of the asphalt-binder. These findings are consistent with the results from temperature sweep tests and further illustrate that the Type II rejuvenator had a poor repeated rejuvenation effect.

When comparing the differences of the MSCR evaluation indices (R and J_{nr}) under the two stress levels shown in Figure 7, the results showed that the differences in $J_{nr0.1}$ and $J_{nr3.2}$ of the rejuvenated asphalt-binders with the Type I and III rejuvenators increased with an increase in the rejuvenation cycles. The discrepancy between $J_{nr0.1}$ and $J_{nr3.2}$ revealed that the stress sensitivity of the asphalt-binder, namely an increasing sensitivity of the rejuvenated SBSMA to the variation of stress loading as the rejuvenation cycles increased. The trend was mainly attributed to the degradation of the SBS polymer in the SBSMA asphalt-binder during the repeated rejuvenation, which weakened the modification effects of the asphalt-binder.

Comparing Figures 7a and 8a, the percentage recovery of the asphalt-binder slightly increased after aging, pointing to improved resistance to permanent deformation. This increase in percentage recovery indicates a potential increase in elasticity of the asphalt-binders due to aging. Figure 7a also shows that under the same stress level, the creep recovery of the asphalt-binder decreased when the rejuvenation cycles increased. This indicates that the addition of the rejuvenators could supplement the viscous component of the asphalt-binder to effectively compensate and delay the aging of the asphalt-binder [36].

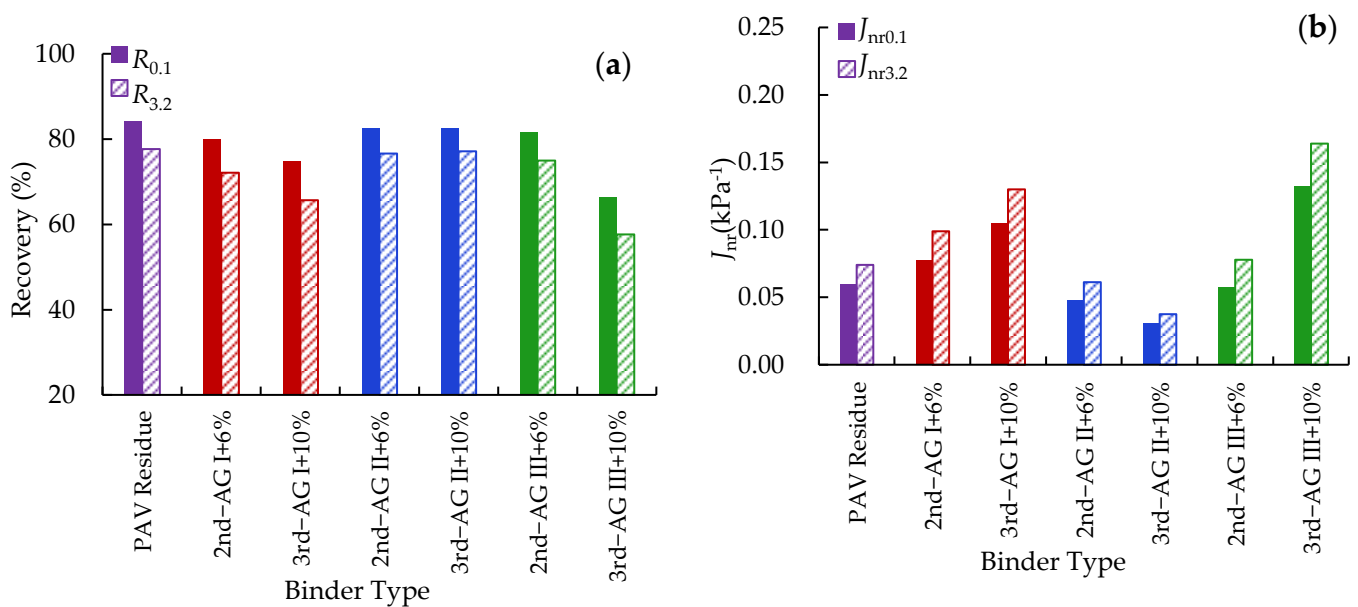


Figure 8. MSCR rutting evaluation of repetitively aged asphalt-binders: (a) recovery; (b) non-recoverable creep compliance (J_{nr}) (Red bars: the asphalt-binders rejuvenated with Type I; blue bars: the asphalt-binders rejuvenated with Type II; green bars: the asphalt-binders rejuvenated with Type III).

Comparing Figures 7b and 8b, it is observed that the non-recoverable creep compliance of the aged asphalt-binder declined significantly. This indicates that aging partly provided an improvement in elasticity and that the elasticity of the asphalt-binders after rejuvenation was obviously restored. With an increase in the aging cycles, the asphalt-binders with Type I and Type III rejuvenators exhibited an increasing trend in J_{nr} , whilst the aged asphalt-binder with Type II exhibited a decreasing trend at 0.1 kPa and 3.2 kPa, respectively (see Figure 8b). Under the same stress level, the superiority ranking of the non-recoverable creep compliance of SBSMA in the equivalent aging cycle was Type I \approx Type III > Type II, and that of SBSMA in the equivalent rejuvenation cycle was Type III > Type I > Type II, respectively.

3.1.3. LAS Analysis

To evaluate the fatigue life (N_f) of the asphalt-binders with the parameters A and B, strain levels of 2.5%, 5%, and 10% were used in this study. The fatigue behavior of the rejuvenated SBSMA significantly depends on the applied strain loading and the rheological property of asphalt-binder as well as the type of rejuvenators. The results in Figure 9 show a significant decrease in the fatigue life of asphalt-binders at elevated strain levels. That is, high strain loading significantly weakened the fatigue resistance of the SBSMA.

At low strain levels, thermal oxidative aging did not appear to significantly affect the fatigue life of the asphalt-binders. In fact, there was an increase in the fatigue life at lower strain levels. However, this was not the case at the 10% strain level. This may be explained from the perspective that the increase in viscosity and stiffness of the asphalt-binder due to aging promoted the asphalt-binders to convert to more linear-elastic behavior at low strain levels with a logical decline in the fatigue life under the adverse effects of aging at high strain levels [37]. As the aging and rejuvenation cycles increased, both the aged and rejuvenated asphalt-binders roughly showed a decreasing trend in fatigue life at the high strain level.

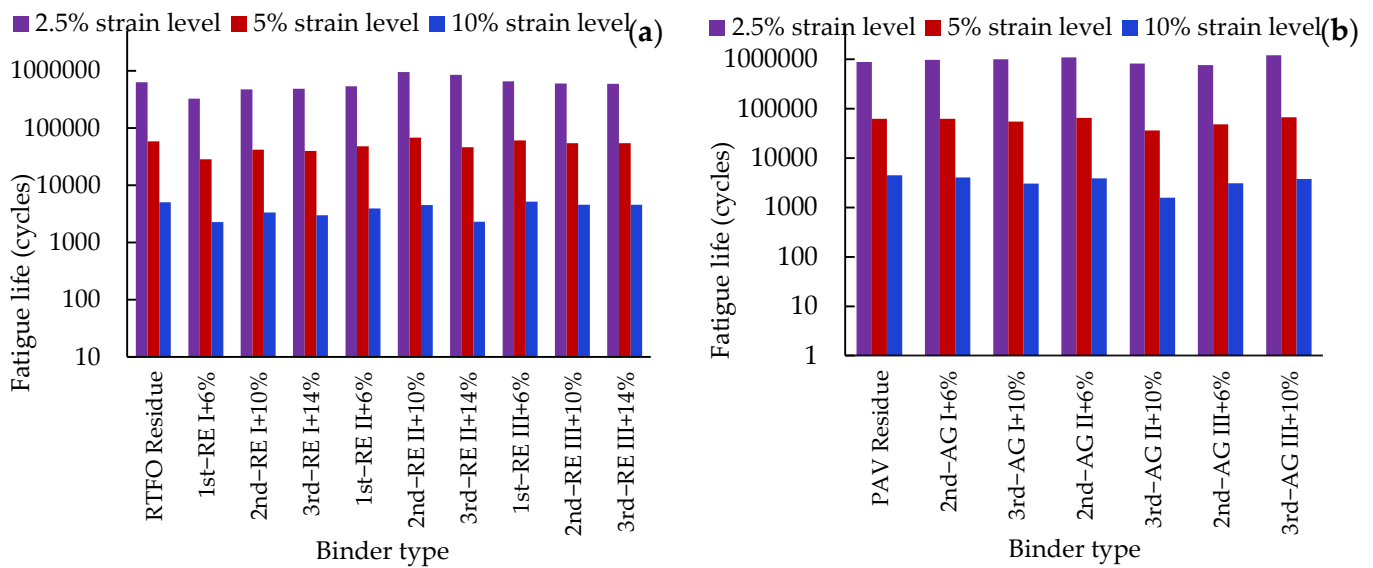


Figure 9. LAS fatigue life results: (a) rejuvenated asphalt-binders; (b) aged asphalt-binders.

3.2. FTIR Analysis

To quantitatively investigate the influence of multiple aging and rejuvenation cycles on the SBSMA chemical structure and the vibration of the functional groups under repeated aging and rejuvenation, the $600\text{--}2000\text{ cm}^{-1}$ functional group peak area was selected as a reference to calculate the butadiene ($\text{CH}=\text{CH}$), carbonyl ($\text{C}=\text{O}$), and sulfoxide ($\text{S}=\text{O}$) relative contents. This helped to eliminate the influence of the thickness and concentration of the asphalt-binders. The chemical aging indices, namely butadiene index (BI), carbonyl index (CI), and sulfoxide index (SI), were determined using Equations (1)–(3) [38]:

$$\text{CI} = \frac{\text{Area of the carbonyl centered around } 1700\text{ cm}^{-1}}{\text{Area of spectral bands between } 2000\text{ and } 600\text{ cm}^{-1}} \quad (1)$$

$$\text{SI} = \frac{\text{Area of the sulfoxide centered around } 1030\text{ cm}^{-1}}{\text{Area of spectral bands between } 2000\text{ and } 600\text{ cm}^{-1}} \quad (2)$$

$$\text{BI} = \frac{\text{Area of the butadiene centered around } 966\text{ cm}^{-1}}{\text{Area of spectral bands between } 2000\text{ and } 600\text{ cm}^{-1}} \quad (3)$$

Figure 10 gives more intuitive information about the changes in the functional groups. As the aging cycles increased, repetitively aged asphalt-binders showed an obviously increasing trend in the CI value. The indistinctive increasing and decreasing trends in the SI and BI values, respectively, are obvious. In the aging process of SBSMA, due to oxidation, dehydrogenation, and cross-linking reactions of the asphalt-binder and SBS polymer, degradation occurred simultaneously, and the spatial network structure was destroyed [39,40]. By comparing the aged and rejuvenated asphalt-binders, it can be seen that the rejuvenating effect was obvious in each aging and rejuvenation cycle, and that the decrease in the BI, CI, and SI values were significant.

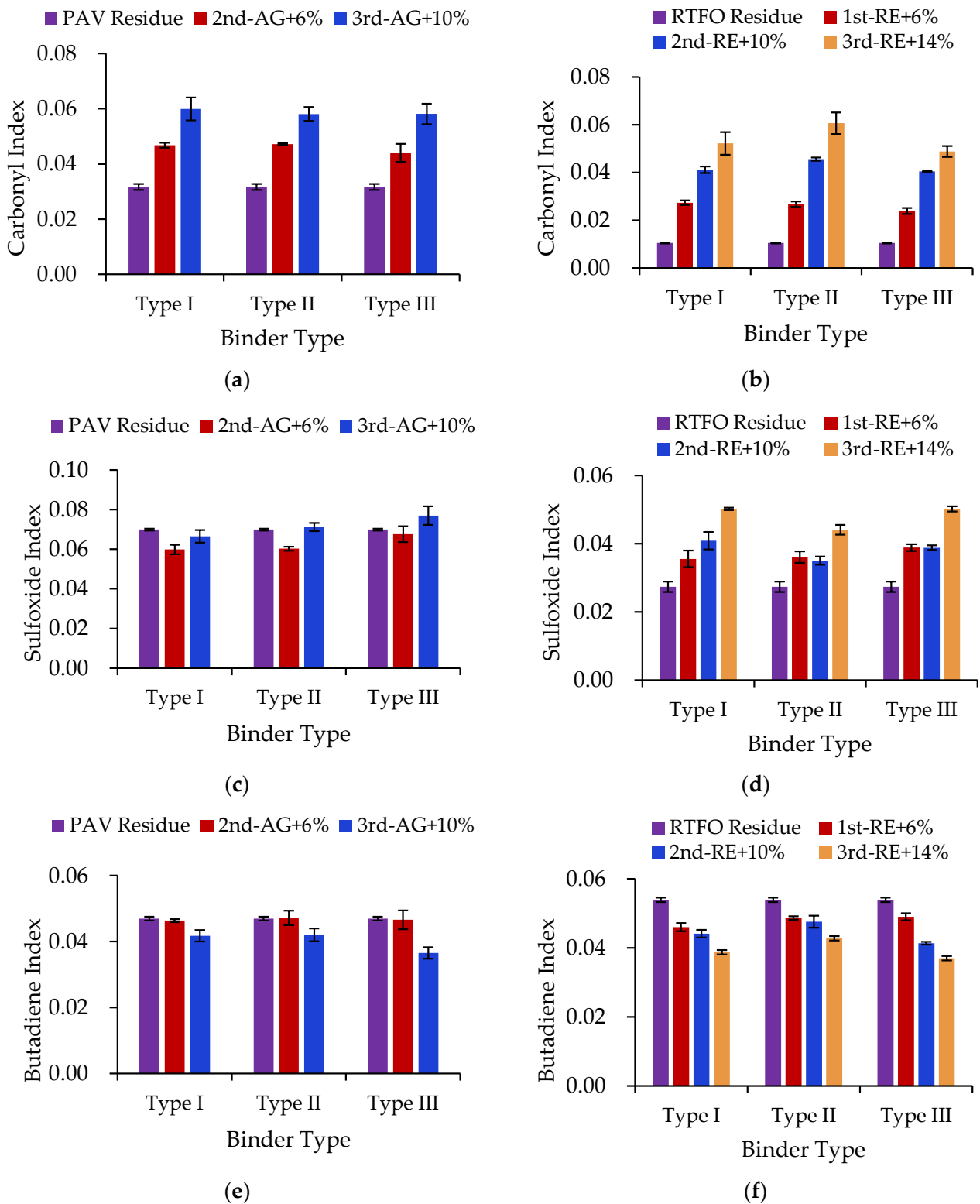


Figure 10. Chemical aging indices of repetitively aged and rejuvenated SBSMA: (a) AG-CI; (b) RE-CI; (c) AG-SI; (d) RE-SI; (e) AG-BI; (f) RE-BI.

Based on the theory of compositional harmonic on rejuvenation mechanisms [41], the rejuvenators rich in aromatics are added to the aged asphalt-binder to dilute the aged asphalt-binders, enhance the proportion of maltenes, and harmonize the different fractions in the asphalt-binder. This was not simply the reversal of the transformation from aromatics

into asphaltenes during the aging process, expressing that the aromatics were consumed and asphaltenes increased.

However, as the dosage of rejuvenators increased in each cycle, the CI and SI values of the rejuvenated asphalt-binders also increased, whilst the value of BI decreased during the repeated aging and rejuvenation cycles. In other words, the aging of the rejuvenated asphalt-binder was faster than the asphalt-binder after RTFO aging. This might be explained by the decrease of the aging resistance due to the oxidative degradation of SBS polymer in the multiple aging process [42]. Meanwhile, the oxidation and breaking of polybutadiene (PB) segments of SBS would produce more oxygen-containing groups such as $-OH$, $C=O$, $-COOH$, etc. [43,44]. Hence, the increased aromatic hydrocarbon oil might have also led to the acceleration of the asphalt-binder aging. The addition of the rejuvenator indicated the potential to improve the rheological properties of the aged asphalt-binders but could not restore the chemical aging indices to the same level as the RTFO residue. As a result, the rejuvenating effect was not significant enough to achieve an appreciable repeated rejuvenation.

With an increase in the rejuvenation cycles, the CI value decreased, especially for the Type III rejuvenator. This indicated that all the three types of rejuvenators had certain rejuvenating effects on the aged asphalt-binders, with the Type III rejuvenator being more impactful. On the other hand, the SI value of the third rejuvenated asphalt-binder with Type II was the smallest while the third rejuvenated asphalt-binder with Types I and III had the largest SI value in magnitude. These results indicated that the Type II rejuvenator was relatively more effective at inhibiting aging of the asphalt-binder. By contrast, the BI value of the rejuvenated asphalt-binder with Type II had the lowest rate of decay, whilst that of the asphalt-binder with Type III declined rapidly. A possible explanation for this could be that the Type II rejuvenator had some chemical components to minimize the SBS degradation, whilst Type III had more maltenes to dilute the contents of SBS [45].

3.3. AFM Analysis

3.3.1. Microstructure of the Asphalt-Binder Surface

By means of the NanoScope Analysis software [46], the AFM height images of various SBSMA asphalt-binders after being subjected to multiple aging and rejuvenation cycles are shown in Figure 11. The roughness indices of the asphalt-binders determined from these images are shown in Figure 12.

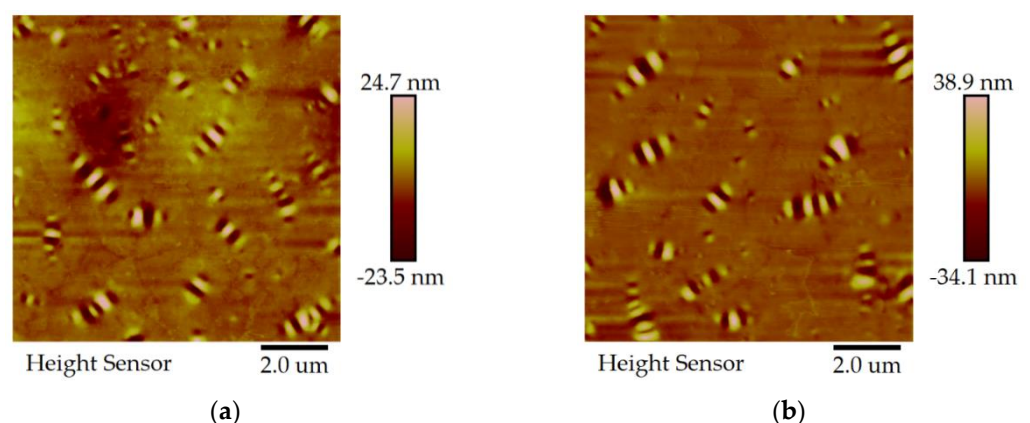


Figure 11. Cont.

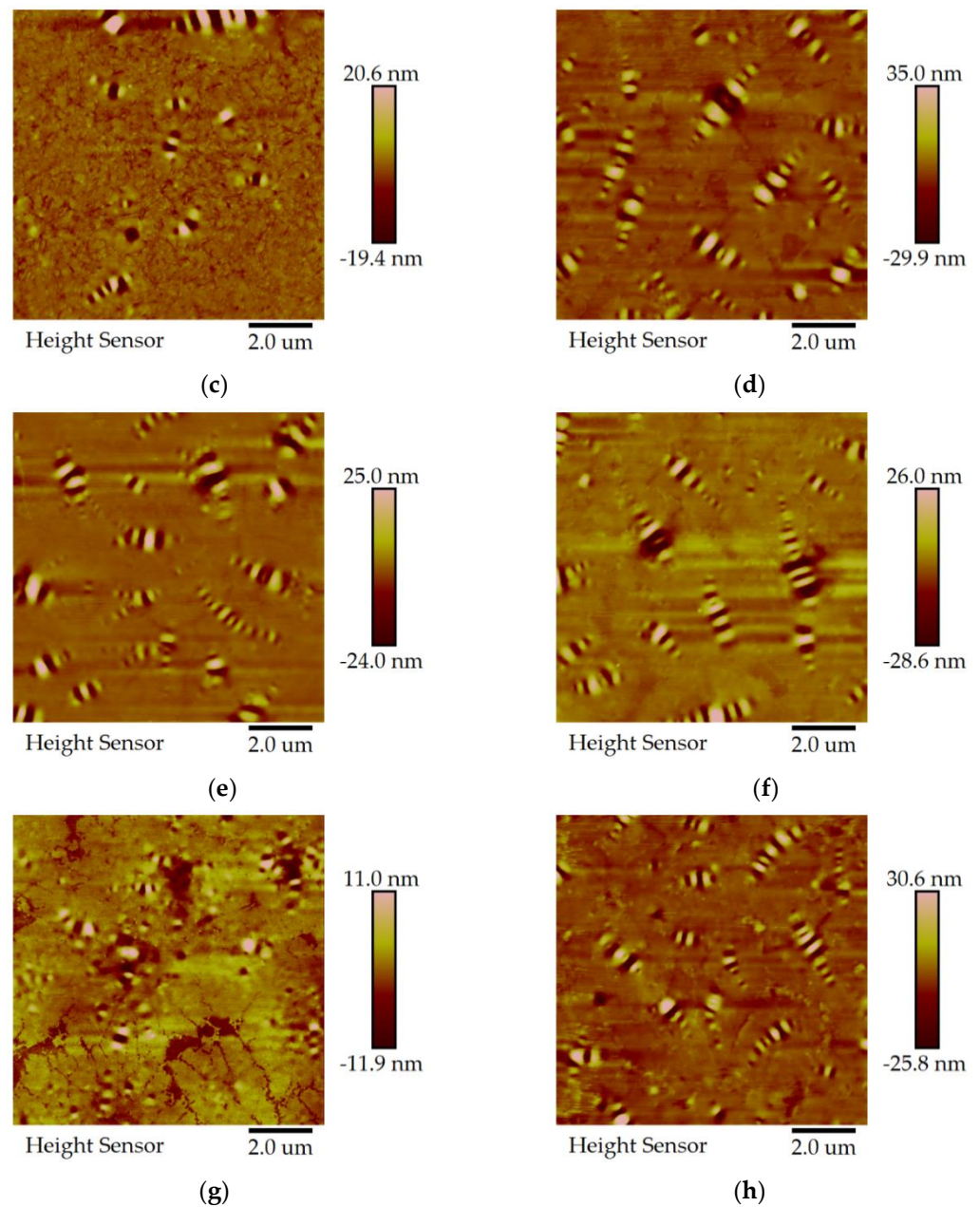


Figure 11. Microstructures obtained from AFM images of the asphalt-binders: (a) Virgin; (b) RTFO Residue; (c) PAV Residue; (d) 1st-RE I + 6%; (e) 2nd-AG I + 6%; (f) 2nd-RE I + 10%; (g) 3rd-AG I+10%; (h) 3rd-RE I + 14%.

Figure 11 shows the two-dimensional (2-D) AFM images of different asphalt-binders subjected to multiple aging and rejuvenation cycles to illustrate the influence of multiple aging and rejuvenation cycles on the microstructure evolution of the asphalt-binder's surface. The appearance of many beelike structures with different sizes could be clearly seen on the surface of the virgin SBSMA (see Figure 11a). After aging, the number of large-sized beelike structures in the PAV residue declined noticeably.

With the addition of the rejuvenator, tiny beelike structures appeared on the rejuvenated asphalt-binder samples with increased morphological undulations. Compared to the asphalt-binder before aging, the size of the beelike structures in the second and third aged asphalt-binders decreased considerably, with the height of the beelike structures increasing as well. By contrast, the quantity, size, and height of the beelike structures of

the second and third rejuvenated asphalt-binder increased substantially. However, the quantity declined in contrast to the asphalt-binder before rejuvenation (see Figure 11d–h).

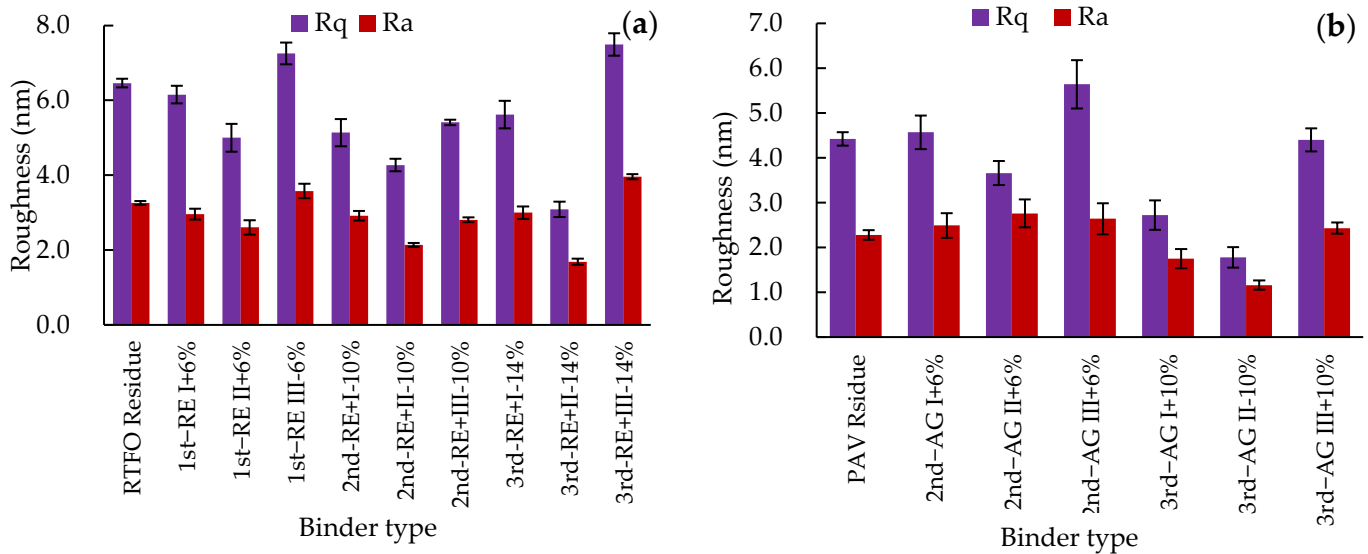


Figure 12. AFM roughness analysis: (a) rejuvenated asphalt-binders; (b) aged asphalt-binders.

3.3.2. Morphological Features of the Asphalt-Binder Surface

The surface roughness indices reflected the degree of development of the beelike structure. Figure 12 shows the roughness indices that were calculated from the height of $30 \times 30 \mu\text{m}$ AFM images. The roughness indices selected for analysis were the average roughness (R_a) and root-mean-square roughness (R_q).

After multiple aging and rejuvenation cycles, the R_a and R_q values of the asphalt-binders with different rejuvenators had a similar response trend. After aging, the R_a and R_q values of the asphalt-binder surface decreased. By contrast, the roughness indices appeared to have been restored after rejuvenation, which is similar to the findings reported by Yu et al. [47]. This could be because the molecular movement of the asphalt-binders decreased after aging, with the accumulation and nucleation of the polar components being hindered. This led to the reduction in the size and height of the beelike structures. The addition of the rejuvenator to supplement maltenes could promote the mobility of the asphalt-binder molecules. Therefore, the size and height of the beelike structures of rejuvenated asphalt-binder were greater than those of the aged asphalt-binder. This helps to explain the mechanism responsible for the formation of the beelike structures during the rejuvenation process.

However, the three rejuvenators showed different rejuvenation effects. The surface of the asphalt-binders with the Type III rejuvenator were the roughest and had the greatest beelike structures in height. The asphalt-binders with the Type II rejuvenator had the least roughness, with the lowest height in the beelike structures. After three rejuvenation cycles, the roughness of the rejuvenated asphalt-binder with Type III was more than twice that of the asphalt-binder with Type II. This might be because the Type III rejuvenator replenished most of the light components and greatly improved the mobility of the maltene molecules. By contrast, Type II only slightly promoted the accumulation of the polar components.

4. Conclusions and Recommendations

This study investigated the effects of the three aging and rejuvenation cycles with three types of rejuvenators designated as Type I, II, and III with different dosages (6%, 10%, and 14%, respectively). The rheological (thermal, rutting, and fatigue resistance), chemical, and morphological characteristics of SBSMA were evaluated using the DSR, LAS, FTIR, and AFM tests. From this study, the following conclusions were drawn:

- The superiority ranking for the rutting factor of the repetitively aged asphalt-binders and fatigue factor of the repetitively rejuvenated asphalt-binders was Type II > Type I > Type III, respectively. Multiple rejuvenation cycles reduced the percentage recovery of the SBSMA with varying rejuvenators and made the asphalt-binder depend more sensitively on the strain levels. The fatigue life of the rejuvenated SBSMA with the three rejuvenators increased at low stress level and decreased at high strain level as the rejuvenation cycles were increased. Considering the high- and intermediate-temperature performance, the Type I rejuvenator exhibited a satisfactory rejuvenation effect.
- From FTIR analysis, the carbonyl and sulfoxide groups of SBSMA increased whilst the chain segments of butadiene decreased after repeated aging and rejuvenation cycles. The addition of the rejuvenator could not restore the chemical aging indices to the same level as the RTFO residue. During the multiple aging and rejuvenation cycles, the aging resistance of SBSMA gradually decreased. This inherently limited the expected rejuvenation effects under the repeated rejuvenation cycles.
- From AFM morphological analysis, PAV aging decreased the quantity of the beelike structures and the surface roughness of the asphalt-binders. The rejuvenators significantly changed the microscopic morphology and phase dispersion of the aged asphalt-binders. The three rejuvenators showed different rejuvenation effects, but generally increased the morphological undulations and surface roughness.

Overall, plausible results were obtained in this laboratory study with promising potential for using rejuvenators to improve the rheological properties of asphalt-binders. The study has also shown that rejuvenators have the potential of achieving satisfactory repeated aging and rejuvenation in terms of performance characteristics (rutting, thermal, and fatigue cracking resistances) and morphological features of SBSMA. Nonetheless, the conclusions drawn are not exhaustive nor exclusive as the test results presented herein pertain to the specific materials evaluated in this study. Future research should include a wide array of different materials including high-activity rejuvenators to further supplement this study's findings including field application trials and validation.

Author Contributions: Conceptualization, X.C. and Y.N.; methodology, Y.N. and J.W.; validation, X.Z. and Y.G.; formal analysis, Y.N. and W.W.; investigation, X.Z.; resources, X.C. and R.Z.; writing—original draft preparation, Y.N. and J.W.; writing—review and editing, X.C. and X.Z.; visualization, Y.N.; supervision, X.C. and J.T.; funding acquisition, Y.G. All authors have read and agreed to the published version of the manuscript.

Funding: This research was funded by the National Science Foundation of China (Grant No. 51778140 and No. 52078130), Suzhou Transport Investment, Planning Design and Management Co., Ltd. (Grant No. 8521008637), and Kunshan Transportation Development Holding Group Co., Ltd. (Grant No. 8521002599 and No. 8521008420).

Institutional Review Board Statement: Not applicable.

Informed Consent Statement: Not applicable.

Data Availability Statement: No new data were created or analyzed in this study. Data sharing is not applicable to this article.

Acknowledgments: The authors would like to acknowledge sincerely the financial support provided by the National Science Foundation of China (Grant No. 51778140 and No. 52078130), Suzhou Transport Investment, Planning Design and Management Co., Ltd. (Grant No. 8521008637), and Kunshan Transportation Development Holding Group Co., Ltd. (Grant No. 8521002599 and No. 8521008420)

for this study. Special thanks and due gratitude go to all those who offered the administrative and technical support during the course of this study.

Conflicts of Interest: The authors declare no conflict of interest.

References

1. Lesueur, D.; Teixeira, A.; Lázaro, M.M.; Andaluz, D.; Ruiz, A. A simple test method in order to assess the effect of mineral fillers on bitumen ageing. *Constr. Build. Mater.* **2016**, *117*, 182–189. [[CrossRef](#)]
2. Ren, S.; Liu, X.; Xu, J.; Lin, P. Investigating the role of swelling-degradation degree of crumb rubber on CR/SBS modified porous asphalt binder and mixture. *Constr. Build. Mater.* **2021**, *300*, 124048. [[CrossRef](#)]
3. Zhu, C.; Zhang, H.; Zhang, D.; Chen, Z. Influence of Base Asphalt and SBS Modifier on the Weathering Aging Behaviors of SBS Modified Asphalt. *J. Mater. Civ. Eng.* **2018**, *30*, 04017306. [[CrossRef](#)]
4. Cong, P.; Guo, X.; Mei, L. Investigation on rejuvenation methods of aged SBS modified asphalt binder. *Fuel* **2020**, *279*, 118556. [[CrossRef](#)]
5. Zeng, W.; Wu, S.; Wen, J.; Chen, Z. The temperature effects in aging index of asphalt during UV aging process. *Constr. Build. Mater.* **2015**, *93*, 1125–1131. [[CrossRef](#)]
6. Ma, T.; Huang, X.; Zhao, Y.; Yuan, H. Aging Behaviour and Mechanism of SBS-Modified Asphalt. *J. Test. Eval.* **2012**, *40*, 20120150. [[CrossRef](#)]
7. Ouyang, C.; Wang, S.; Zhang, Y.; Zhang, Y. Improving the aging resistance of styrene–butadiene–styrene tri-block copolymer modified asphalt by addition of antioxidants. *Polym. Degrad. Stab.* **2006**, *91*, 795–804. [[CrossRef](#)]
8. Tauste, R.; Moreno-Navarro, F.; Sol-Sánchez, M.; Rubio-Gámez, M.C. Understanding the bitumen ageing phenomenon: A review. *Constr. Build. Mater.* **2018**, *192*, 593–609. [[CrossRef](#)]
9. Wang, Z.; Ye, F. Experimental investigation on aging characteristics of asphalt based on rheological properties. *Constr. Build. Mater.* **2020**, *231*, 117158. [[CrossRef](#)]
10. Xu, J.; Sun, L.; Pei, J.; Xue, B.; Liu, T.; Li, R. Microstructural, chemical and rheological evaluation on oxidative aging effect of SBS polymer modified asphalt. *Constr. Build. Mater.* **2021**, *267*, 121028. [[CrossRef](#)]
11. Cuciniello, G.; Leandri, P.; Filippi, S.; Lo Presti, D.; Polacco, G.; Losa, M.; Airey, G. Microstructure and rheological response of laboratory-aged SBS-modified bitumens. *Road Mater. Pavement Des.* **2021**, *22*, 372–396. [[CrossRef](#)]
12. Huang, M.; Dong, Q.; Ni, F.; Wang, L. LCA and LCCA based multi-objective optimization of pavement maintenance. *J. Clean. Prod.* **2021**, *283*, 124583. [[CrossRef](#)]
13. Jiang, H.; Zhang, J.; Sun, C.; Liu, S.; Liang, M.; Yao, Z. Experimental assessment on engineering properties of aged bitumen incorporating a developed rejuvenator. *Constr. Build. Mater.* **2018**, *179*, 1–10. [[CrossRef](#)]
14. Behnood, A. Application of rejuvenators to improve the rheological and mechanical properties of asphalt binders and mixtures: A review. *J. Clean. Prod.* **2019**, *231*, 171–182. [[CrossRef](#)]
15. Yao, H.; Dai, Q.; You, Z. Fourier Transform Infrared Spectroscopy characterization of aging-related properties of original and nano-modified asphalt binders. *Constr. Build. Mater.* **2015**, *101*, 1078–1087. [[CrossRef](#)]
16. Yan, C.; Huang, W.; Ma, J.; Xu, J.; Lv, Q.; Lin, P. Characterizing the SBS polymer degradation within high content polymer modified asphalt using ATR-FTIR. *Constr. Build. Mater.* **2020**, *233*, 117708. [[CrossRef](#)]
17. Zhao, X.; Wang, S.; Wang, Q.; Yao, H. Rheological and structural evolution of SBS modified asphalts under natural weathering. *Fuel* **2016**, *184*, 242–247. [[CrossRef](#)]
18. Feng, Z.; Cai, F.; Yao, D.; Li, X. Aging properties of ultraviolet absorber/SBS modified bitumen based on FTIR analysis. *Constr. Build. Mater.* **2021**, *273*, 121713. [[CrossRef](#)]
19. Lin, P.; Liu, X.; Apostolidis, P.; Erkens, S.; Zhang, Y.; Ren, S. ESEM observation and rheological analysis of rejuvenated SBS modified bitumen. *Mater. Des.* **2021**, *204*, 109639. [[CrossRef](#)]
20. Yang, Z.; Zhang, X.; Zhang, Z.; Zou, B.; Zhu, Z.; Lu, G.; Xu, W.; Yu, J.; Yu, H. Effect of Aging on Chemical and Rheological Properties of Bitumen. *Polymers* **2018**, *10*, 1345. [[CrossRef](#)]
21. Zhu, H.; Xu, G.; Gong, M.; Yang, J. Recycling long-term-aged asphalts using bio-binder/plasticizer-based rejuvenator. *Constr. Build. Mater.* **2017**, *147*, 117–129. [[CrossRef](#)]
22. Guo, M.; Liang, M.; Jiao, Y.; Tan, Y.; Yu, J.; Luo, D. Effect of aging and rejuvenation on adhesion properties of modified asphalt binder based on AFM. *J. Microsc.* **2021**. [[CrossRef](#)] [[PubMed](#)]
23. Kaya Ozdemir, D.; Topal, A.; McNally, T. Relationship between microstructure and phase morphology of SBS modified bitumen with processing parameters studied using atomic force microscopy. *Constr. Build. Mater.* **2021**, *268*, 121061. [[CrossRef](#)]
24. Cong, P.; Liu, N.; Tian, Y.; Zhang, Y. Effects of long-term aging on the properties of asphalt binder containing diatoms. *Constr. Build. Mater.* **2016**, *123*, 534–540. [[CrossRef](#)]
25. Aghazadeh Dokandari, P.; Topal, A.; Kaya Ozdemir, D. Rheological and Microstructural Investigation of the Effects of Rejuvenators on Reclaimed Asphalt Pavement Bitumen by DSR and AFM. *Int. J. Civ. Eng.* **2021**, *19*, 749–758. [[CrossRef](#)]
26. Chen, X.; Wang, J.; Zhang, X.; Liu, H.; Tong, J.; Zhao, R. Evaluating the Physical and Rheological Properties of Rejuvenated Styrene-Butadiene-Styrene-Modified Asphalt Binders. *Adv. Mater. Sci. Eng.* **2020**, *2020*, 1–14. [[CrossRef](#)]
27. Grilli, A.; Gnisci, M.L.; Bocci, M. Effect of ageing process on bitumen and rejuvenated bitumen. *Constr. Build. Mater.* **2017**, *136*, 474–481. [[CrossRef](#)]

28. Qian, Y.; Guo, F.; Leng, Z.; Zhang, Y.; Yu, H. Simulation of the field aging of asphalt binders in different reclaimed asphalt (RAP) materials in Hong Kong through laboratory tests. *Constr. Build. Mater.* **2020**, *265*, 120651. [[CrossRef](#)]
29. *ASTM D2872: Standard Test Method for Effect of Heat and Air on a Moving Film of Asphalt (Rolling Thin-Film Oven Test)*; ASTM International: West Conshohocken, PA, USA, 2019.
30. *ASTM D6521: Standard Practice for Accelerated Aging of Asphalt Binder Using a Pressurized Aging Vessel*; ASTM International: West Conshohocken, PA, USA, 2019.
31. *ASTM D7405: Standard Test Method for Multiple Stress Creep and Recovery (MSCR) of Asphalt Binder Using a Dynamic Shear Rheometer*; ASTM International: West Conshohocken, PA, USA, 2015.
32. *AASHTO T391-20: Standard Method of Test for Estimating Fatigue Resistance of Asphalt Binders Using the Linear Amplitude Sweep*; American Association of State Highway and Transportation Office: Washington, DC, USA, 2020.
33. Ren, R.; Han, K.; Zhao, P.; Shi, J.; Zhao, L.; Gao, D.; Zhang, Z.; Yang, Z. Identification of asphalt fingerprints based on ATR-FTIR spectroscopy and principal component-linear discriminant analysis. *Constr. Build. Mater.* **2019**, *198*, 662–668. [[CrossRef](#)]
34. Zhang, J.; Simate, G.S.; Hu, X.; Souliman, M.; Walubita, L.F. Impact of recycled asphalt materials on asphalt binder properties and rutting and cracking performance of plant-produced mixtures. *Constr. Build. Mater.* **2017**, *155*, 654–663. [[CrossRef](#)]
35. Kataware, A.V.; Singh, D. A study on rutting susceptibility of asphalt binders at high stresses using MSCR test. *Innov. Infrastruct. Solut.* **2017**, *2*, 4. [[CrossRef](#)]
36. Zhong, H.; Huang, W.; Yan, C.; Zhang, Y.; Lv, Q.; Sun, L.; Liu, L. Investigating binder aging during hot in-place recycling (HIR) of asphalt pavement. *Constr. Build. Mater.* **2021**, *276*, 122188. [[CrossRef](#)]
37. Ziari, H.; Amini, A.; Goli, A. The effect of different aging conditions and strain levels on relationship between fatigue life of asphalt binders and mixtures. *Constr. Build. Mater.* **2020**, *244*, 118345. [[CrossRef](#)]
38. Zhao, Y.; Gu, F.; Xu, J.; Jin, J. Analysis of Aging Mechanism of SBS Polymer Modified Asphalt based on Fourier Transform Infrared Spectrum. *J. Wuhan Univ. Technol. Mater. Sci. Ed.* **2010**, *25*, 1047–1052. [[CrossRef](#)]
39. Cortizo, M.S.; Larsen, D.O.; Bianchetto, H.; Alessandrini, J.L. Effect of the thermal degradation of SBS copolymers during the ageing of modified asphalts. *Polym. Degrad. Stab.* **2004**, *86*, 275–282. [[CrossRef](#)]
40. Li, Y.; Li, L.; Zhang, Y.; Zhao, S.; Xie, L.; Yao, S. Improving the aging resistance of styrene-butadiene-styrene tri-block copolymer and application in polymer-modified asphalt. *J. Appl. Polym. Sci.* **2010**, *116*, 754–761. [[CrossRef](#)]
41. Kuang, D.; Liu, W.; Xiao, Y.; Wan, M.; Yang, L.; Chen, H. Study on the rejuvenating mechanism in aged asphalt binder with mono-component modified rejuvenators. *Constr. Build. Mater.* **2019**, *223*, 986–993. [[CrossRef](#)]
42. Hao, G.; Huang, W.; Yuan, J.; Tang, N.; Xiao, F. Effect of aging on chemical and rheological properties of SBS modified asphalt with different compositions. *Constr. Build. Mater.* **2017**, *156*, 902–910. [[CrossRef](#)]
43. Xu, X.; Yu, J.; Xue, L.; Zhang, C.; Zha, Y.; Gu, Y. Investigation of Molecular Structure and Thermal Properties of Thermo-Oxidative Aged SBS in Blends and Their Relations. *Materials* **2017**, *10*, 768. [[CrossRef](#)] [[PubMed](#)]
44. Cao, Z.; Chen, M.; Yu, J.; Han, X. Preparation and characterization of active rejuvenated SBS modified bitumen for the sustainable development of high-grade asphalt pavement. *J. Clean. Prod.* **2020**, *273*, 123012. [[CrossRef](#)]
45. Cao, X.; Wang, H.; Cao, X.; Sun, W.; Zhu, H.; Tang, B. Investigation of Rheological and Chemical Properties Asphalt Binder Rejuvenated with Waste Vegetable Oil. *Constr. Build. Mater.* **2018**, *180*, 455–463. [[CrossRef](#)]
46. Ding, L.; Wang, X.; Zhang, M.; Chen, Z.; Meng, J.; Shao, X. Morphology and properties changes of virgin and aged asphalt after fusion. *Constr. Build. Mater.* **2021**, *291*, 123284. [[CrossRef](#)]
47. Yu, X.; Zauamanis, M.; dos Santos, S.; Poulikakos, L.D. Rheological, microscopic, and chemical characterization of the rejuvenating effect on asphalt binders. *Fuel* **2014**, *135*, 162–171. [[CrossRef](#)]